Unfolding of Alanine-Based Peptides Using Electron Spin Resonance Distance Measurements†

Sangmi Jun, James S. Becker, Mike Yonkunas, Rob Coalson, and Sunil Saxena*

Department of Chemistry, University of Pittsburgh, Pittsburgh, Pennsylvania 15260

Received June 15, 2006; Revised Manuscript Received August 2, 2006

ABSTRACT: We describe a scheme for tagging an alanine-based peptide with a Cu(II) and a nitroxide to measure unfolding transitions. The enhancement in longitudinal relaxation rate of the nitroxide due to the presence of Cu(II) was measured at physiological temperatures by pulsed electron spin resonance (ESR). The change in relaxation rate provided the average interspin distance between the Cu(II) and the nitroxide. Control experiments on a proline-based peptide verify the robustness of the method. The change in interspin distances with temperature for the alanine-based peptide is in accord with the change in helicity measured by circular dichroism. The data provide an opportunity to examine the unfolding process in polyalanine peptides. The distance in the folded state is in concordance with molecular dynamics. However, the ESR experiment measures an average distance of 17 Å in the unfolded state, whereas molecular dynamics indicates a distance of 42 Å if the unfolded geometry was a polyproline type II helix. Therefore, ESR demonstrates that the unfolded state of this alanine-based peptide is not an ideal *extended* polyproline type II helix.

The advent of site-directed spin labeling has resulted in electron spin resonance (ESR)[1] emerging as a useful spectroscopic technique for the measurement of protein structure and conformational dynamics (*1*−*4*). Using site-directed spin labeling, two spin labels (typically nitroxides) can be placed at virtually any position on the protein backbone. Concomitant methodological developments in ESR (*5*−*12*) permit the measurement of interspin distance in the range of 8−70 Å in order to provide constraints for structure elucidations (*13*−*26*). However, the distance methods are largely applicable only at very low temperatures (ca. 10−80 K), and this proves to be a disadvantage in the context of monitoring unfolding events in proteins or peptides.

We describe an approach by which distances of at least up to 25 Å can be measured using ESR at physiologically relevant temperatures. In this approach a Cu(II) binding site is generated at one end of a biomolecule. A nitroxide spin label is attached at another position using site-directed spin labeling. By exploiting methodological advances in Fourier transform ESR (*12*, *27*−*33*) which enable the routine measurement of the free induction decay signal from labeled macromolecules, the enhancement of relaxation rate of the nitroxide by the presence of Cu(II) is obtained. The enhancement of relaxation rate can be used to measure metal to nitroxide interspin distances, as has been well demonstrated at low temperatures (*34*−*39*). We show that nanometer range interspin distances may also be measured at physiological temperatures. This builds on methodologies developed by Voss et al. (*40*), which showed that the changes in nitroxide line broadening and intensity may be used to measure the metal−nitroxide distance. Nitroxide−nitroxide distances at physiological temperatures may also be measured by calibrating the increase in the line broadening due to the presence of the second spin (*41*).

Significantly, we show that this methodology may be used to resolve the average distance between two units as an alanine-based peptide melts with temperature. Thus the experiments capture the average separation between two units in the ensemble of conformations that constitute a given step in the unfolding pathway. The unfolding transition of polyalanines is of paradigmatic significance in the field of protein folding. Spectroscopic experiments (*42*−*48*) as well as computer simulations (*42*, *44*, *49*−*51*) have recently indicated that α-helical polyalanine peptides unfold to polyproline type-II helical structures (PPII). This geometry has also been suggested to exist in the unfolded states of other peptides (*52*, *53*) and some proteins (*52*, *54*, *55*). This is significant because, if such nativelike secondary structure elements are indeed present in the unfolded state of proteins, then the entropic cost associated with folding is vastly reduced. Our results support the conclusions of Pande and co-workers that the PPII geometry of individual alanines does not propagate into an overall *extended* polyproline II structure in the unfolded state of polyalanines (*56*).

MATERIALS AND METHODS

Sample Preparation. The alanine-based peptide PPHGGG-WPAAAAKAAAAKCAAAAKA (P, proline; H, histidine; G, glycine; W, tryptophan; A, alanine; K, lysine; C, cysteine), shown schematically in Figure 1, and the proline-based peptide PPHGGGWPPPPPPPCPPK were synthesized at the

† The research was supported by an NSF Career grant (MCB 0346898).

* To whom correspondence should be addressed. Phone: (412) 624-8680. Fax: (412) 624-8611. E-mail: sksaxena@pitt.edu.

[1] Abbreviations: CD, circular dichroism; CHARMM, *c*hemistry at *har*vard *m*olecular *m*echanics; CW, continuous wave; ESR, electron spin resonance; FID, free induction decay; FRET, fluorescence resonance energy transfer; MD, molecular dynamics; MM3, molecular mechanics force field; MTSSL, (1-oxy-2,2,5,5-tetramethylpyrroline-3-methyl)methanethiosulfonate spin label; NEM, *N*-ethylmorpholine; NMR, nuclear magnetic resonance; PME, particle mesh Ewald; PPII, polyproline type II helix; SDSL, site-directed spin labeling; UV, ultraviolet; VMD, visual molecular dynamics.

10.1021/bi061195b CCC: $33.50
Published on Web 09/02/2006

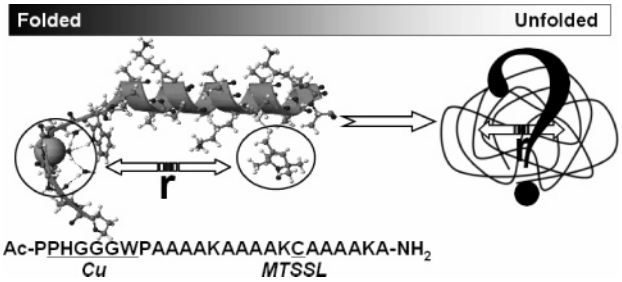

FIGURE 1: The central question of the state to which a polyalanine helix unfolds is illustrated. A schematic of the folded α-helical state of polyalanine is shown on the left. The Cu(II) center and the nitroxide spin label are also shown. The ESR experiments measure the interspin distance between Cu(II) and nitroxide, *r*, as a function of temperature.

Molecular Medicine Institute, University of Pittsburgh. In these peptides, the lysine residues serve to confer solubility in aqueous solutions, and the PHGGGW sequence constitutes a well-characterized copper binding sequence (*57*−*59*). Using site-directed spin labeling (SDSL), a (1-oxy-2,2,5,5-tetramethylpyrroline-3-methyl)methanethiosulfonate spin label (MTSSL) that was purchased from Toronto Research Chemicals Inc. (Ontario, Canada) was covalently bound to the cysteine residue in both peptides.

For ESR experiments, 250 μM solutions of each peptide were prepared in an aqueous buffered solution of 10 mM potassium chloride (KCl) and 25 mM *N*-ethylmorpholine (NEM), at pH 7.6. Spectroscopic data were obtained on each peptide in the presence and in the absence of coordinated Cu(II). Experiments were also conducted in the presence of Zn(II), a diamagnetic metal. For the metal-coordinated samples, a 1 mol equiv of Cu(II) [or Zn(II)] was added from a 0.01 M aqueous copper sulfate (or zinc chloride) solution. For ESR experiments, 6 μL of peptide solution in a 1.5 mm inner diameter Pyrex tube was degassed by freeze−pump−thaw cycles until a final pressure of 2×10^{-4} Torr to eliminate oxygen in the solution. The samples were bath sonicated for approximately 5 min before insertion into the ESR cavity.

Electron Spin Resonance (ESR) Spectroscopy. Spectroscopic experiments were performed on a Bruker EleXsys E580 X-band CW/Pulse ESR spectrometer equipped with a Bruker ER4118X-MS3 split-ring resonator. The temperature was controlled using an Oxford 1TC605 temperature controller and an Oxford ER 4118CF gas flow cryostat.

The longitudinal relaxation time of the nitroxide in the peptide samples was measured over a temperature range of 270−315 K by using an inversion recovery sequence. The inversion recovery experiment consists of a two-pulse, $\pi-t-\pi/2$ sequence. The high output power of the ASE-TWTA (1 kW) combined with a quality factor, *Q*, much less than 100 provided $\pi/2$ and π pulses of 6 and 12 ns, respectively. The initial interpulse separation, *t*, was 20 ns, and the delay *t* was stepped out by 180−340 ns for a total 64 or 128 points according to each experimental condition. The FID after the second pulse was digitized every 4 ns for a total of 1024 points after a dead time of 50 ns. At each temperature, the experimental data were measured several times, and the errors were determined from the standard deviation of these measurements.

Circular Dichroism (CD) Spectroscopy. The thermal stability of the peptides was assessed using CD by following the change in the spectrum with temperature. The peptides were dissolved in a 10 mM potassium phosphate buffer, a pH of 7.0, and at a peptide concentration of 250 μM. The measurements were made on an AVIV model 202 circular dichroism spectrometer. The samples contained 400 μL of peptide solution in a 0.1 cm path-length cuvette. A single wavelength, 220 nm, which measures the net α-helicity, was monitored for the alanine-based peptide as a function of temperature (*60*). The data for the peptide in the presence and absence of Cu(II) were practically identical (see Supporting Information), indicating that Cu(II) binding does not substantially change the thermodynamics of thermal unfolding. For the proline-based peptide, a wavelength of 206 nm, which monitors the net polyproline II (PPII) helical structure, was monitored (*61*, *62*). The signals at the specific wavelength were then recorded continuously as the temperature was increased from 268 to 368 K, with sampling points at every 1 K.

The affinity of peptide−Cu(II) complexes was verified by CD. When Cu(II) binds to peptides, weak d−d transitions appear in the visible region over a range of wavelengths from 500 to 750 nm (*57*). According to the CD data Cu(II) was bound to the peptide between 270 and 365 K. On the basis of the affinities of Cu(II) to the HGGGW segments (*57*), as much as 88% of the peptides bind Cu(II). A simple analysis shows that the incomplete binding leads to errors of less than 0.5 Å in the measured distances.

Generation of α-Helical and PPII Ensembles. To define the α-helical conformation, the peptide without the copper binding domain (AAAAKAAAAKCAAAAKA) was constructed with Ramachandran angles, Φ and Ψ of −57° and −47°, for peptide angles Φ and Ψ, respectively. For the extended polyproline II (PPII) conformation, these angles were modified to $\Phi = -75°$ and $\Psi = 145°$ to reflect an ideal polyproline II helical-type geometry. The copper binding domain (PPHGGGW) coordinates were obtained from the X-ray structure (*58*) and joined to the backbone through the added proline residue Pro-8. The dihedral angle Ψ between Pro-8 and Ala-9, joining the copper binding domain to the peptide, was energy minimized using the molecular mechanics (MM3) force field (*63*). Dihedrals angles of $\Psi = -28°$ and $\Psi = 46°$ were obtained for the α-helical and PPII-type ensembles, respectively.

A new residue was added to the CHARMM27 force field (*64*) representing the MTSSL spin label attached to a modified cysteine residue side chain. The bonds, angles, and dihedrals of the spin label were modeled according to previous research on nitroxides (*65*). In the same light, charges on MTSSL were selected on the basis of CHARMM standards and modeled from the CHARMM27 amino acid force field. Two systems were prepared for molecular dynamics (MD) simulations: the alanine-based peptide in the α-helical conformation and the same peptide in the PPII conformation, both built up with a Cys-19-MTSSL side chain substitution. Each system was solvated in the VMD molecular graphics environment (*66*) utilizing the built-in solvate 1.2 package. The solvent box was extended to 7 Å beyond the largest dimension along each axis. This condition allows minimal protein−protein interaction upon generation of periodic boundaries during simulations. All atom simulations were performed using the NAMD2 package (*67*). A conjugate gradient energy minimization was performed over 10000

steps to relieve bad contacts, with a harmonic protein backbone restraint of 999 kcal mol^{-1} Å^{-2}. The α-helical system was then subjected to a short equilibration at 300 K and the PPII system at 315 K for 100 ps at constant volume. Subsequently, 250 ps of constant pressure molecular dynamics was performed with the protein backbone restrained to 500 kcal mol^{-1} Å^{-2}. Langevin dynamics and Langevin piston pressure (*68*) were used to maintain temperature and pressure at 300 or 315 K and 1 bar, respectively. Periodic boundary conditions and all atom wrapping were imposed for all simulations. Long-range electrostatics was calculated with the particle mesh Ewald (PME) formalism and updated every four steps. A time step of 1 fs was used with trajectories written every 0.5 ps. A van der Waals cutoff distance of 10 Å and a pair list distance of 11.5 Å were implemented at each phase of dynamics simulations.

Tcl scripting in VMD was used to determine the average distance over all trajectory frames from the copper atom to the nitroxide spin label for each simulation system. Average distances converged to a value of 25 and 42 Å for the α-helical conformation and the PPII conformation, respectively, after 100−200 ps of MD simulations.

RESULTS AND DISCUSSION

The alanine-based peptide (PPHGGGWPAAAAKAAAAK-CAAAAKA) and the proline-based peptide (PPHGGGWP-PPPPPPCPPK) were designed with a Cu(II) binding PHGGGW sequence at one end (*57*−*59*). In both, a nitroxide spin label was covalently attached to the cysteine using site-directed spin labeling (*3*, *4*, *69*, *70*). Transition metals, such as Cu(II), usually have a much shorter longitudinal relaxation time than the nitroxyl radical. In systems containing a nitroxide and a coordinated transition metal, the fast relaxing metal spin can enhance the rate of the relaxation of the more slowly relaxing nitroxide spin (*35*, *71*, *72*). The change in the relaxation rate of the nitroxide depends on r^{-6}, where r is the average distance between Cu(II) and nitroxyl spin. Eaton and co-workers have demonstrated the usefulness of this effect to determine the interspin distances between an Fe(III) center and nitroxide in complexes of metmyoglobin variants and methemoglobin (*37*−*39*) at low temperature (ca. 10−170 K).

Methodological advances in ESR now permit the detection of the Fourier transform ESR signal even for samples with transverse relaxation times of ∼20 ns (*12*, *28*, *30*−*32*), as is typical for spin-labeled peptides and proteins. Thus the nitroxide relaxation times can be measured even at physiological temperatures. We show that by monitoring the change in nitroxide relaxation time upon coordination of the peptide with Cu(II), the distance, r, can be measured as the polyalanine peptide melts with temperature.

Figure 2 shows the inversion recovery experimental data at 305 K for the alanine-based peptide in the absence of Cu(II) (Figure 2a) and in the presence of Cu(II) (Figure 2b). In Figure 2, the frequency dimension (ν) provides the continuous wave (CW) equivalent spectrum and the time dimension (denoted by t) illustrates the recovery of magnetization to equilibrium after inversion of magnetization with a π pulse. The recovery of magnetization for the three hyperfine components of the nitroxide can be obtained by extracting slices parallel to "t" from the 2-D data set. The data for the central component are shown in the insets of Figure 2.

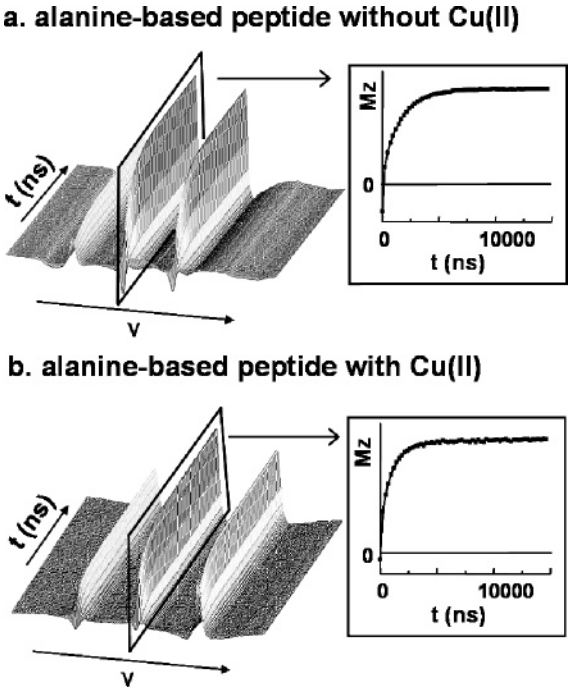

FIGURE 2: Inversion recovery spectrum of the nitroxide in the alanine-based peptide (a) without Cu(II) and (b) with Cu(II) at 305 K, respectively. The recovery curves for the central component are shown in the insets.

For the central nitroxide line the recovery of magnetization depends on the rate of electron spin-flips as well as on the rate of nuclear spin-flips. Schwartz and Freed (*73*) analyzed this effect theoretically, and they found that, in general, the recovery obeys a biexponential behavior of the form (*73*, *74*):

$$S(t) = A + B\exp(-t/T_{1s}) + C\exp(-t/T_A) \qquad (1)$$

where $S(t)$ is the signal from the inversion recovery experiment, T_{1s} is the electron longitudinal relaxation time, and T_A depends on the nuclear spin-flip rates. The first time constant, T_{1s}, is related to electron spin-flips [note that subsequently we will use T_{1s}^0 and T_{1s} to denote the nitroxide longitudinal relaxation times in the absence and in the presence of Cu(II), respectively]. Schwartz and Freed found that T_A decreases from the slow motional regime to the fast motional regime, and finally T_A becomes constant in the fast motional regime (*73*).

All experimental recovery curves for both peptides fit well to eq 1. The value of T_A was constant at 120 ns throughout the entire experimental temperature region, as expected from theory (*73*, *74*) for data in the fast motional regime. Figure 3 shows the longitudinal relaxation rates for the alanine-based peptide with Cu(II) and without Cu(II) between 270 and 314 K. As control, the longitudinal relaxation rates for the peptide in the presence of Zn(II) (a diamagnetic metal) are also shown. In the presence of coordinated Zn(II), the nitroxide relaxation rate of the peptide does not change dramatically, demonstrating that the metal binding to the peptide does not change the peptide hydrodynamic radius. On the other hand, the nitroxide relaxation rate in the alanine-based peptide is enhanced by the addition of copper ion (a paramagnetic metal). The enhancement upon addition of Cu(II) is 11% at 270 K and 53% at 314 K, indicating that the average distance, r, decreases as the helix melts.

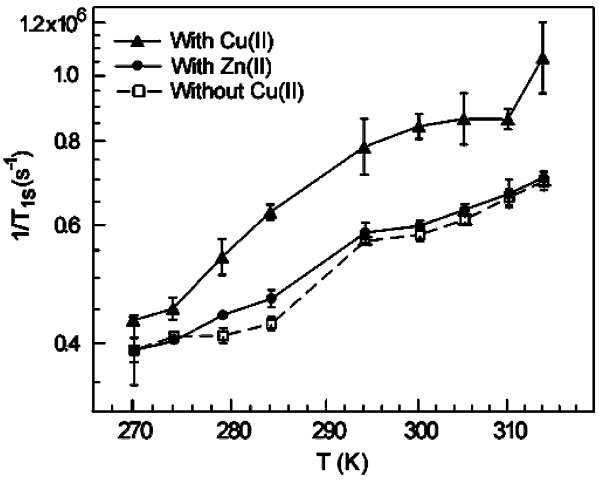

FIGURE 3: Nitroxide longitudinal relaxation rates of the alanine-based peptide in the absence (squares) and presence of Cu(II) (triangles) and in the presence of Zn(II) (circles). At each temperature, the longitudinal relaxation time was measured several times, and the error values were determined from the standard deviation. Addition of Cu(II), a paramagnetic metal, enhances the rate of the relaxation.

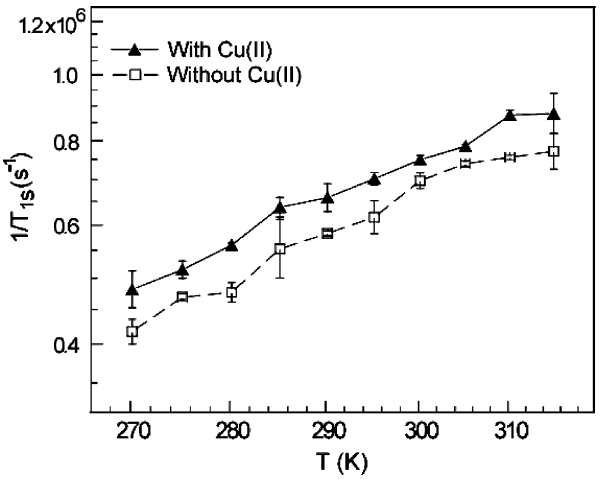

FIGURE 4: Nitroxide longitudinal relaxation rates of the proline-based peptide in the absence and presence of Cu(II). Enhancement in relaxation rate due to addition of Cu(II) is fairly constant.

In Figure 4, the nitroxide relaxation rate for the proline-based peptide in the absence and presence of Cu(II) is shown as a function of temperature. The relaxation rate increases from 270 to 315 K, but the enhancement in nitroxide relaxation is fairly constant over the temperature range. At 270 K the enhancement upon addition of Cu(II) is 15%, and at 315 K it is 14%, indicating that the average distance, *r*, remains fairly constant over this temperature range.

Quantitative estimates of *r* for the two peptides may be obtained by using the Bloembergen theory (*75*−*77*) as modified by Kulikov and Likhtenshtein for application to systems containing a nitroxide and a paramagnetic metal (*35*, *71*, *72*). For the case of Cu(II) and in the fast motional regime:

$$r = \left(\frac{g_s^2 g_f^2 \beta_e^4}{10\hbar^2}\left[\frac{T_{2f}}{1+(\omega_f-\omega_s)^2 T_{2f}^2} + \frac{3T_{1f}}{1+\omega_s^2 T_{1f}^2} + \frac{6T_{2f}}{1+(\omega_f+\omega_s)^2 T_{2f}^2}\right]\right)^{1/6}\left[\frac{1}{T_{1s}} - \frac{1}{T_{1s}^0}\right]^{-1/6} \quad (2)$$

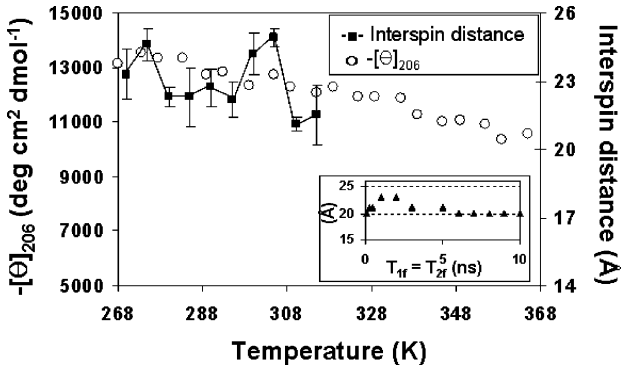

FIGURE 5: The Cu(II)−nitroxide interspin distances for the proline-based peptide from 270 to 315 K overlaid on the thermal unfolding profile for proline-based peptide obtained using CD. Change of the interspin distance at 285 K as a function of T_{1f} ($=T_{2f}$) is shown in the inset.

where *r* is the average interspin distance between Cu(II) and nitroxide, and *f* and *s* denote the electron spin of Cu(II) and nitroxide, respectively. The parameter T_{1s}^0 is the electronic longitudinal relaxation time of the nitroxide in the absence of Cu(II), and T_{1s} is the longitudinal relaxation time of the nitroxide in the presence of Cu(II). The parameters T_{1f} and T_{2f} are the electronic longitudinal and transverse relaxation times, respectively, for Cu(II). In eq 2, the values of g_f and g_s, which represent the *g* factors for Cu(II) and nitroxide electron spins, are 2.1166 (*78*) and 2.0061 (*32*, *79*). Also, ω_f and ω_s, the resonant frequencies for Cu(II) and nitroxide, are 10.162 and 9.6317 GHz. Finally, β_e is the Bohr magneton and $\hbar$ is the Planck constant (*h*) divided by 2π.

Equation 2 is strictly valid under the condition $\mu_0 g_s g_f \beta_e^2 T_{1f}/(4\pi h r^3) \ll 1$. Using a T_{1f} of 3 ns (see below), the constant yields 0.03 at $r = 17$ Å and 0.01 at $r = 25$ Å, respectively, demonstrating that eq 2 can be used for the distance range measured in the two peptides (see below). In principle, modulation of the electron−electron dipolar interaction by rotational tumbling of the peptide could also contribute to the enhancement of relaxation. However, estimates of the enhancement based on this effect overpredict the experimental enhancements, indicating that this model is incorrect (see Supporting Information). The distance estimates based on eq 2 are also in good agreement with molecular modeling in the folded state of the peptide and with fluorescence results in the folded and unfolded states (*80*).

The values of $[1/T_{1s} - 1/T_{1s}^0]$ are determined experimentally (cf. Figures 3 and 4). To determine *r*, the values of T_{1f}, T_{2f} [the longitudinal and transverse relaxation times for Cu(II)] are required. Although $T_{1f} \approx T_{2f}$ in the fast motional regime, the parameters T_{1f}, T_{2f} are, in principle, temperature dependent. However, the data on the proline-based peptide suggest that for this coordination geometry T_{1f}, T_{2f} are constant over the measured temperature range.

Equation 2 was used to estimate the distance *r* for the proline-based peptide using the assumption that T_{1f} and T_{2f} are constant. In the analysis a value of $T_{1f} = T_{2f} = 3$ ns as reported in the literature (*81*, *82*) was used. Figure 5 shows the measured distance *r* overlaid on the CD data for the proline-based peptide. The CD data indicate that the net PPII structure is fairly stable over this temperature range. Over the temperature range *r* changes from 24 to 21 Å, which is consistent with the stability of the PPII structure as indicated

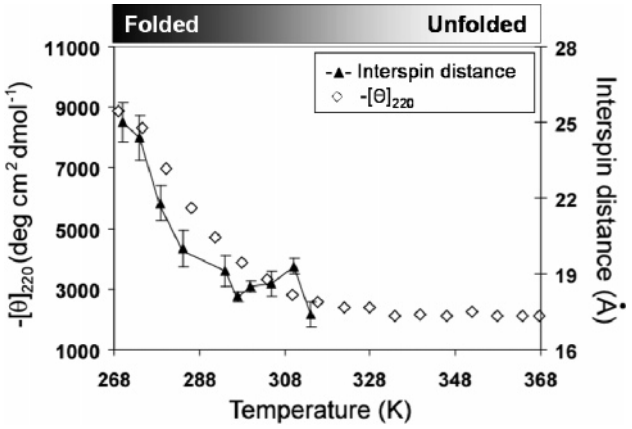

FIGURE 6: Cu(II)−nitroxide interspin distances for the alanine-based peptide from 270 to 314 K overlaid on the thermal unfolding profile for the alanine-based peptide measured using CD.

by CD. The measured value of r is also relatively insensitive to the exact value of T_{1f}. Changing the value of T_{1f} ($=T_{2f}$) over 2 orders of magnitude (i.e., from 0.1 to 10 ns) in eq 2 affects the obtained distance, r, by less than 10%. This is illustrated in the inset of Figure 5, which plots the interspin distance at 285 K as a function of T_{1f} ($=T_{2f}$). An average interspin distance of ∼22−24 Å for proline-based peptide is also in accord with single molecule fluorescence and molecular dynamics results on polyproline peptides (*83*). Thus the assumption that $T_{1f} = T_{2f} = 3$ ns over the temperature range is reasonable.

Thus, the change in r for the alanine-based peptide as it melts can be determined by using $T_{1f} = T_{2f} = 3$ ns in eq 2. Figure 6 shows the CD data and the ESR determined Cu(II)−nitroxide interspin distances in the alanine-based peptide. The CD data indicate that the α-helicity is greatest at the lowest temperature and decreases as the temperature is increased. The change in interspin distances is clearly in concordance with the change in helicity indicated by CD. As temperature increases, the Cu(II)−nitroxide interspin distance in the alanine-based peptide decreases from 25 ± 0.8 Å at 270 K to 17 ± 0.5 Å at 314 K, respectively. When the relaxation rates of the peptide with Zn(II) were used for $1/T_{1s}^0$ in eq 2, the Cu(II)−nitroxide interspin distances are within experimental errors at all temperatures except at 279 K. At this temperature the Cu(II)−nitroxide distance was found to be 21.8 ± 0.7 Å with the Zn(II) data instead of 20.8 ± 0.5 Å. The errors are estimated from experimental errors in the measurement of T_{1s} from multiple measurements and reflect uncertainties in the measurement of the mean distance. The sample is characterized by a distribution in distance due to the flexibility in the linker as well as the peptide backbone; the errors do not reflect the width of this distribution. Since the ESR observable (i.e., the change in relaxation rate) depends on r^{-6}, the ESR measured average distance is biased toward shorter conformations. In the Supporting Information we provide estimates of this bias for this peptide using the assumption that the range of distances in the unfolded state is described by a Gaussian. The difference between the measured average distance from ESR and the actual mean distance is estimated to be within 7−20% for these peptides as long as the standard deviation of the distribution is within 4 Å.

Significantly, we have been able to resolve the change in average distance as an alanine-based peptide melts with temperature. Each step of the folding pathway is encompassed by an ensemble of conformations, and these experiments capture the average separation between two units at each step. To infer the structural implications of these distances, we generated several ensembles with the polyalanine segments in α-helical conformations and in extended PPII conformations (cf. Materials and Methods section). The average interspin distance in the α-helical ensembles was found to be ∼25 Å, which is in good agreement with the experimental interspin distance of ∼25 Å in the folded state of this alanine-based peptide. In the unfolded state, the ESR-measured interspin distance was ∼17 Å. Using single molecule fluorescence resonance energy transfer (FRET), Gnanakaran et al. (*80*) measured the average end-to-end distance of the 20-residue alanine-based peptide to be ∼30 Å in the folded α-helical conformation and ∼23 Å in the unfolded state. The decrease of average distance upon unfolding observed by the FRET experiments is in agreement with the ESR results. The discrepancies in the actual distances are possibly due to differences in the amino acid sequences and in the lengths of the fluorescence tag versus the chelating residues.

The average distance should increase if the unfolded state of the alanine-based segment is in an extended PPII geometry. In fact, the average interspin distance in the PPII conformation in the molecular models is ∼42 Å, which is not consistent with the experimental interspin distance of ∼17 Å in the unfolded state. The presence of a distribution in distances is not sufficient to explain this discrepancy (see Supporting Information). Experimental evidence from NMR and UV Raman indicates that individual alanine residues sample Φ and Ψ Ramachandran angles close to those corresponding to a PPII conformation (*44*, *45*, *48*). However, the ESR experiments demonstrate that the PPII geometry does not propagate into an overall extended fold, at least over 10 amino acid residues. This is consistent with recent small-angle X-ray scattering results, which found that the radius of gyration of an unfolded polyalanine peptide is about 40% lower than that expected of an extended PPII helix (*56*). Our experiments, however, do not rule out the possibility that the PPII geometry might extend over shorter stretches of amino acids. Future experiments which systematically scan the nitroxide along the chain will directly shed light on this issue. While useful in resolving the global structure of the peptides in the unfolded state, the experimental data cannot measure the full distribution in distances. Therefore, the experimental variation of average distances could not be used to provide further insight into the preferred model of folding (see Supporting Information).

These results also address a critical need for ESR techniques that can measure nanometer scale distances at physiological temperatures. The experiments build on recent research that measured interspin distances by calibrating the nitroxide line broadening and line intensity due to interaction with a lanthanide (*84*), a paramagnetic metal (*40*, *81*, *85*), or another nitroxide (*41*). The distinct advantage of the continuous wave approaches is that widely available instrumentation and simple analysis can be used. The pulsed ESR results described in this paper are, nevertheless, encouraging. First, the method retains the advantage of a relatively

straightforward analysis (*35*−*39*). Second, extension to larger distances might be possible given the enhanced sensitivity of FT-ESR to small changes in relaxation rates (especially homogeneous line widths). Third, the results describe an application of ESR to monitor unfolding transition in model peptides. They can be extended to more complicated folding processes in metalloproteins, as long as information on the relaxation rate of the metal is available. It is also instructive to compare this technique to fluorescence resonance energy transfer (FRET). While FRET can be sensitive to energy transfer over a larger length scale (ca. 10−12 nm), recent single molecule fluorescence results (*83*) clearly indicate that molecular reorientations must be accounted for properly, to correctly interpret this energy transfer in terms of distances, even for polyproline peptides.

SUMMARY

We describe a scheme for tagging a biomolecule with a Cu(II) and a nitroxide to measure the unfolding transition. We show that the enhancement in longitudinal relaxation rate of the nitroxide due to the presence of Cu(II) can be measured at physiological temperatures using Fourier transfrom ESR. The change in relaxation rate can be used to measure the interspin distance between the Cu(II) and the nitroxide. Data on a proline-based peptide, which forms a stable PPII-type structure, illustrate the robustness of the method. In the alanine-based peptide, the average interspin distance between Cu(II) and nitroxide decreases from 25 Å in the folded α-helical state to 17 Å in the unfolded state. The data show that the unfolded state of this alanine-based peptide is not an ideal *extended* PPII geometry.

ACKNOWLEDGMENT

We thank Prof. Sanford Asher for many helpful discussions.

SUPPORTING INFORMATION AVAILABLE

Details about the data analysis procedures, expanded discussions, and circular dichroism data. This material is available free of charge via the Internet at http://pubs.acs.org.

REFERENCES

1. Altenbach, C., Marti, T., Khorana, H. G., and Hubbell, W. L. (1990) Transmembrane protein structure: spin labeling of bacteriorhodopsin mutants, *Science 248*, 1088−1092.
2. Hubbell, W. L., Gross, A., Langen, R., and Lietzow, M. A. (1998) Recent advances in site-directed spin labeling of proteins, *Curr. Opin. Struct. Biol. 8*, 649−656.
3. Hubbell, W. L., Cafiso, D. S., and Altenbach, C. (2000) Identifying conformational changes with site-directed spin labeling, *Nat. Struct. Biol. 7*, 735−739.
4. Columbus, L., and Hubbell, W. L. (2002) A new spin on protein dynamics, *Trends Biochem. Sci. 27*, 288−295.
5. Larson, R. G., and Singel, D. J. (1993) Double electron-electron resonance spin-echo modulation spectroscopic measurement of electron-spin pair separations in orientationally disordered solids, *J. Chem. Phys. 98*, 5134−5146.
6. Rabenstein, M. D., and Shin, Y. K. (1995) Determination of the distance between spin labels attached to a macromolecule, *Proc. Natl. Acad. Sci. U.S.A. 92*, 8239−8243.
7. Saxena, S., and Freed, J. H. (1997) Theory of double quantum two-dimensional electron spin resonance with application to distance measurements, *J. Chem. Phys. 107*, 1317−1340.
8. Martin, R. E., Pannier, M., Diederich, F., Gramlich, V., Hubrich, H., and Spiess, H. W. (1998) Determination of end-to-end distances in a series of TEMPO diradicals of up to 2.8 nm length with a new four-pulse double electron electron resonance experiment, *Angew. Chem., Int. Ed. 37*, 2834−2837.
9. Borbat, P. P., and Freed, J. H. (1999) Multiple quantum ESR and distance measurements, *Chem. Phys. Lett. 313*, 145−154.
10. Jeschke, G., Pannier, M., Godt, A., and Spiess, H. W. (2000) Dipolar spectroscopy and spin alignment in electron paramagnetic resonance, *Chem. Phys. Lett. 331*, 243−252.
11. Milov, A. D., Tsvetkov, Y. D., Formaggio, F., Crisma, M., Toniolo, C., and Raap, J. (2000) Self-Assembling properties of membrane-modifying peptides studied by PELDOR and CW-ESR spectroscopies, *J. Am. Chem. Soc. 122*, 3843−3848.
12. Borbat, P. P., Costa-Filho, A. J., Earle, K. A., Moscicki, J. K., and Freed, J. H. (2001) Electron spin resonance in studies of membranes and proteins, *Science 291*, 266−269.
13. Eaton, S. S., Moore, K. M., Sawant, B. M., and Eaton, G. R. (1983) Use of the EPR half-field transition to determine the interspin distance and orientation of the interspin vector in systems of two unpaired electrons, *J. Am. Chem. Soc. 105*, 6560−6567.
14. Hustedt, E. J., and Beth, A. H. (1999) Nitroxide spin-spin interactions: Applications to protein structure and dynamics, *Annu. Rev. Biophys. Biomol. Struct. 28*, 129−153.
15. Pannier, M., Schadler, V., Schops, M., Wiesner, U., Jeschke, G., and Spiess, H. W. (2000) Determination of ion cluster sizes and cluster-to-cluster distances in ionomers by four-pulse double electron-electron resonance, *Macromolecules 33*, 7812−7818.
16. Altenbach, C., Oh, K.-J., Trabanino, R. J., Hideg, K., and Hubbell, W. L. (2001) Estimation of inter-residue distances in spin labeled proteins at physiological temperatures: Experimental strategies and practical limitations, *Biochemistry 40*, 15471−15482.
17. Milov, A. D., Tsvetkov, Y. D., Formaggio, F., Crisma, M., Toniolo, C., and Raap, J. (2001) The secondary structure of a membrane-modifying peptide in a supramolecular assembly studied by PELDOR and CW-ESR spectroscopies, *J. Am. Chem. Soc. 123*, 3784−3789.
18. Liu, Y.-S., Sompornpisut, P., and Perozo, E. (2001) Structure of the KcsA channel intracellular gate in the open state, *Nat. Struct. Biol. 8*, 883−887.
19. Perozo, E., Cortes, D. M., Sompornpisut, P., Kloda, A., and Martinac, B. (2002) Open channel structure of MscI and the gating mechanism of mechanosensitive channels, *Nature 418*, 942−948.
20. Borbat, P. P., Mchourab, H. S., and Freed, J. H. (2002) Protein structure determination using long-distance constraints from double-quantum coherence ESR: Study of T4 lysozyme, *J. Am. Chem. Soc. 124*, 5304−5314.
21. Schiemann, O., Weber, A., Edwards, T., Prisner, T., and Sigurdsson, S. (2003) Nanometer distance measurements on RNA using PELDOR, *J. Am. Chem. Soc. 125*, 3434−3435.
22. Kweon, D.-H., Kim, C. S., and Shin, Y.-K. (2003) Regulation of neuronal SNARE assembly by the membrane, *Nat. Struct. Biol. 10*, 440−447.
23. Bonora, M., Becker, J. S., and Saxena, S. (2004) Suppression of electron spin-echo envelope modulation peaks in double quantum coherence electron spin resonance, *J. Magn. Reson. 170*, 278−283.
24. Borbat, P. P., Davis, J. H., Butcher, S. E., and Freed, J. H. (2004) Measurement of large distances in biomolecules using double-quantum filtered refocused electron spin-echoes, *J. Am. Chem. Soc. 126*, 7746−7747.
25. Schiemann, O., Piton, N., Mu, Y., Stock, G., Engels, J. W., and Prisner, T. F. (2004) A PELDOR-based nanometer distance ruler for oligonucleotides, *J. Am. Chem. Soc. 126*, 5722−5729.
26. Xu, Y., Zhang, F., Su, Z., McNew, J. A., and Shin, Y.-K. (2005) Hemifusion in SNARE-mediated membrane fusion, *Nat. Struct. Mol. Biol. 12*, 417−422.
27. Subczynski, W. K., Hyde, J. S., and Kusumi, A. (1989) Oxygen permeability of phosphatidylcholine−cholesterol membranes, *Proc. Natl. Acad. Sci. U.S.A. 86*, 4474−4478.
28. Borbat, P. P., Crepeau, R. H., and Freed, J. H. (1997) Multifrequency two-dimensional Fourier transform ESR: An X/Ku-band spectrometer, *J. Magn. Reson. 127*, 155−167.
29. Subczynski, W. K., Pasenkiewicz-Gierula, M., McElhaney, R. N., Hyde, J. S., and Kusumi, A. (2003) Molecular dynamics of 1-palmitoyl-2-oleoylphosphatidylcholine membranes containing transmembrane-helical peptides with alternating leucine and alanine residues, *Biochemistry 42*, 3939−3948.
30. Costa-Filho, A. J., Shimoyama, Y., and Freed, J. H. (2003) A 2D-ELDOR study of the liquid ordered phase in multilamellar vesicle membranes, *Biophys. J. 84*, 2619−2633.

31. Costa-Filho, A. J., Crepeau, R. H., Borbat, P. P., Ge, M., and Freed, J. H. (2003) Lipid-gramicidin interactions: Dynamic structure of the boundary lipid by 2D-ELDOR, *Biophys. J. 84*, 3364−3378.
32. Bonora, M., Pornsuwan, S., and Saxena, S. (2004) Nitroxide-relaxation over the entire motional range, *J. Phys. Chem. B 108*, 4196−4198.
33. Nielsen, R. D., Che, K., Gelb, M. H., and Robinson, B. H. (2005) A ruler for determining the position of proteins in membranes, *J. Am. Chem. Soc. 127*, 6430−6442.
34. Milov, A. D., Salikhov, K. M., and Tsvetkov, Y. D. (1972) Spin-lattice relaxation of hydrogen atoms and paramagnetic ions in glassy aqueous solutions of sulfuric acid at 77 °K, *Fiz. Tverd. Tela 14*, 2211−2215.
35. Kulikov, A. V., and Likhtenshtein, G. I. (1977) The use of spin relaxation phenomena in the investigation of the structure of model and biological systems by the method of spin labels, *Adv. Mol. Relax. Interact. Proc. 10*, 47−69.
36. Rakowsky, M. H., More, K. M., Kulikov, A. V., Eaton, G. R., and Eaton, S. S. (1995) Time-domain electron paramagnetic resonance as a probe of electron-electron spin-spin interaction in spin-labeled low-spin iron porphyrins, *J. Am. Chem. Soc. 117*, 2049−2057.
37. Rakowsky, M. H., Zecevic, A., Eaton, G. R., and Eaton, S. S. (1998) Determination of high-spin iron(III)-nitroxyl distances in spin-labeled porphyrins by time-domain EPR, *J. Magn. Reson. 131*, 97−110.
38. Seiter, M., Budker, V., Du, J.-L., Eaton, G. R., and Eaton, S. S. (1998) Interspin distances determined by time domain EPR of spin-labeled high-spin methemoglobin, *Inorg. Chim. Acta 273*, 354−366.
39. Zhou, Y., Bowler, B. E., Lynch, K., Eaton, S. S., and Eaton, G. R. (2000) Interspin distances in spin-labeled metmyoglobin variants determined by saturation recovery EPR, *Biophys. J. 79*, 1039−1052.
40. Voss, J., Hubbell, W. L., and Kaback, H. R. (1995) Distance determination in proteins using designed metal ion binding sites and site-directed spin labeling: application to the lactose permease of *Escherichia coli*, *Proc. Natl. Acad. Sci. U.S.A. 92*, 12300−12303.
41. Mchaourab, H. S., Oh, K. J., Fang, C. J., and Hubbell, W. L. (1997) Conformation of T4 lysozyme in solution. Hinge-bending motion and the substrate-induced conformational transition studied by site-directed spin labeling, *Biochemistry 36*, 307−316.
42. Pappu, R. V., and Rose, G. D. (2002) A simple model for polyproline II structure in unfolded states of alanine-based peptides, *Protein Sci. 11*, 2437−2455.
43. Eker, F., Cao, X., Nafie, L., and Schweitzer-Stenner, R. (2002) Tripeptides adopt stable structures in water. A combined polarized visible Raman, FTIR, and VCD spectroscopy study, *J. Am. Chem. Soc. 124*, 14330−14341.
44. Shi, Z., Olson, C. A., Rose, G. D., Baldwin, R. L., and Kallenbach, N. R. (2002) Polyproline II structure in a sequence of seven alanine residues, *Proc. Natl. Acad. Sci. U.S.A. 99*, 9190−9195.
45. Maiti, N. C., Apetri, M. M., Zagorski, M. G., Carey, P. R., and Anderson, V. E. (2004) Raman spectroscopic characterization of secondary structure in natively unfolded proteins: alpha-synuclein, *J. Am. Chem. Soc. 126*, 2399−2408.
46. Schweitzer-Stenner, R., Eker, F., Griebenow, K., Cao, X., and Nafie, L. A. (2004) The conformation of tetraalanine in water determined by polarized Raman, FT-IR, and VCD spectroscopy, *J. Am. Chem. Soc. 126*, 2768−2776.
47. Eker, F., Griebenow, K., Cao, X., Nafie, L. A., and Schweitzer-Stenner, R. (2004) Preferred peptide backbone conformations in the unfolded state revealed by the structure analysis of alanine-based (AXA) tripeptides in aqueous solution, *Proc. Natl. Acad. Sci. U.S.A. 101*, 10054−10059.
48. Asher, S. A., Mikhonin, A. V., and Bykov, S. (2004) UV Raman demonstrates that alpha-helical polyalanine peptides melt to polyproline II conformations, *J. Am. Chem. Soc. 126*, 8433−8440.
49. Zaman, M. H., Shen, M.-Y., Berry, R. S., Freed, K. F., and Sosnick, T. R. (2003) Investigations into sequence and conformational dependence of backbone entropy, inter-basin dynamics and the Flory isolated-pair hypothesis for peptides, *J. Mol. Biol. 331*, 693−711.
50. Mu, Y., Kosov, D. S., and Stock, G. (2003) Conformational dynamics of trialanine in water. 2. Comparison of AMBER, CHARMM, GROMOS, and OPLS force fields to NMR and infrared experiments, *J. Phys. Chem. B 107*, 5064−5073.
51. Garcia, A. E. (2004) Characterization of non-alpha helical conformations in Ala peptides, *Polymer 45*, 669−676.
52. Smyth, E., Syme, C. D., Blanch, E. W., Hecht, L., Vasak, M., and Barron, L. D. (2001) Solution structure of native proteins with irregular folds from Raman optical activity, *Biopolymers 58*, 138−151.
53. Rucker, A. L., and Creamer, T. P. (2002) Polyproline II helical structure in protein unfolded states: Lysine peptides revisited, *Protein Sci. 11*, 980−985.
54. Tiffany, M. L., and Krimm, S. (1968) New chain conformations of poly(glutamic acid) and polylysine, *Biopolymers 6*, 1379−1382.
55. Woody, R. W. (1992) Circular dichroism and conformation of unordered polypeptides, *Adv. Biophys. Chem. 2*, 37−79.
56. Zagrovic, B., Lipfert, J., Sorin, E. J., Millett, I. S., vanGunsteren, W. F., Doniach, S., and Pande, V. S. (2005) Unusual compactness of a polyproline type II structure, *Proc. Natl. Acad. Sci. U.S.A. 102*, 11698−11703.
57. Aronoff-Spencer, E., Burns, C. S., Avdievich, N. I., Gerfen, G. J., Peisach, J., Antholine, W. E., Ball, H. L., Cohen, F. E., Prusiner, S. B., and Millhauser, G. L. (2000) Identification of the Cu^{2+} binding sites in the N-terminal domain of the Prion protein by EPR and CD spectroscopy, *Biochemistry 39*, 13760−13771.
58. Burns, C. S., Aronoff-Spencer, E., Dunham, C. M., Lario, P., Avdievich, N. I., Antholine, W. E., Olmstead, M. M., Vrielink, A., Gerfen, G. J., Peisach, J., Scott, W. G., and Millhauser, G. L. (2002) Molecular features of the copper binding sites in the octarepeat domain of the Prion protein, *Biochemistry 41*, 3991−4001.
59. Millhauser, G. L. (2004) Copper binding in the prion protein, *Acc. Chem. Res. 37*, 79−85.
60. Holzwarth, G., and Doty, P. (1965) The ultraviolet circular dichroism of polypeptides, *J. Am. Chem. Soc. 87*, 218−228.
61. Young, M. A., and Pysh, E. S. (1975) Vacuum ultraviolet circular dichroism of poly(L-proline) I and II, *J. Am. Chem. Soc. 97*, 5100−5103.
62. Kelly, M. A., Chellgren, B. W., Rucker, A. L., Troutman, J. M., Fried, M. G., Miller, A.-F., and Creamer, T. P. (2001) Host-guest study of left-handed polyproline II helix formation, *Biochemistry 40*, 14376−14383.
63. Lii, J. H., and Allinger, N. L. (1991) The MM3 force field for amides, polypeptides and proteins, *J. Comput. Chem. 12*, 186−199.
64. MacKerell, A. D. (1998) 216th ACS National Meeting of the American Chemical Society, Boston, MA.
65. Barone, V., Bencini, A., Cossi, M., Matteo, A. D., Mattesini, M., and Totti, F. (1998) Assessment of a combined QM/MM approach for the study of large nitroxide systems in vacuo and in condensed phases, *J. Am. Chem. Soc. 120*, 7069−7078.
66. Humphrey, W., Dalke, A., and Schulten, K. (1996) VMD: visual molecular dynamics, *J. Mol. Graphics 14*, 33−38.
67. Kale, L., Skeel, R., Bhandarkar, M., Brunner, R., Gursoy, A., Krawetz, N., Phillips, J., Shinozaki, A., Varadarajan, K., and Schulten, K. (1999) NAMD2: Greater scalability for parallel molecular dynamics, *J. Comput. Phys. 151*, 283−312.
68. Hoover, W. G. (1985) Canonical dynamics: Equilibrium phase-space distributions, *Phys. Rev. A 31*, 1695−1697.
69. Millhauser, G. L. (1992) Selective placement of electron spin labels: new structural methods for peptides and proteins, *Trends Biochem. Sci. 17*, 448−452.
70. Gaponenko, V., Howarth, J. W., Columbus, L., Gasmi-Seabrook, G., Yuan, J., Hubbell, W. L., and Rosevear, P. R. (2000) Protein global fold determination using site-directed spin and isotope labeling, *Protein Sci. 9*, 302−309.
71. Kulikov, A. V., and Likhtenshtein, G. I. (1974) Use of saturation curves for evaluating distances in biological objects by the method of double spin labels, *Biofizika 19*, 420−424.
72. Kulikov, A. V. (1976) Determination of the distance between the spins of the spin-label and paramagnetic center in spin-labeled proteins from the saturation curve parameters of EPR spectra of the labels at 77 K, *Mol. Biol. (Moscow) 10*, 132−141.
73. Schwartz, L. J., Millhauser, G. L., and Freed, J. H. (1986) Two-dimensional electron spin-echoes: Magnetization transfer and molecular dynamics, *Chem. Phys. Lett. 127*, 60−66.
74. Schwartz, L. J. (1984) Ph.D. Thesis in Chemistry, Cornell University, Ithaca, NY.

75. Bloembergen, N., Purcell, E. M., and Pound, R. V. (1948) Relaxation effects in nuclear magnetic resonance absorption, *Phys. Rev. 73*, 679−712.
76. Bloembergen, N. (1949) On the interaction of nuclear spins in a crystalline lattice, *Physica 15*, 386-426.
77. Bloembergen, N., Shapiro, S., Pershan, P. S., and Artman, J. O. (1959) Cross-relaxation in spin system, *Phys. Rev. 114*, 445−459.
78. Becker, J. S., and Saxena, S. (2005) Double quantum coherence electron spin resonance on coupled Cu(II)-Cu(II) spins, *Chem. Phys. Lett. 414*, 248−252.
79. Lee, S., Budil, D. E., and Freed, J. H. (1994) Theory of two-dimensional Fourier-transform electron spin resonance for ordered and viscous fluids, *J. Chem. Phys. 101*, 5529−5558.
80. Gnanakaran, S., Hochstrasser, R. M., and Garcia, A. E. (2004) Nature of structural inhomogeneities on folding a helix and their influence on spectral measurements, *Proc. Natl. Acad. Sci. U.S.A. 101*, 9229−9234.
81. Voss, J., Salwinski, L., Kaback, H. R., and Hubbell, W. L. (1995) A method for distance determination in proteins using a designed metal ion binding site and site-directed spin labeling: Evaluation with T4 lysozyme, *Proc. Natl. Acad. Sci. U.S.A. 92*, 12295−12299.
82. Eaton, S. S., and Eaton, G. R. (2000) Relaxation times of organic radicals and transition metal ions, in *Distance Measurements in Biological Systems by EPR* (Berliner, L. J., Eaton, S. S., and Eaton, G. R., Eds.) pp 29−154, Kluwer Academic/Plenum Publisher, New York.
83. Schuler, B., Lipman, E. A., Steinbach, P. J., Kumke, M., and Eaton, W. A. (2005) Polyproline and the "spectroscopic ruler" revisited with single-molecule fluorescence, *Proc. Natl. Acad. Sci. U.S.A. 102*, 2754−2759.
84. Voss, J., Wu, J., Hubbell, W. L., Jacques, V., Meares, C. F., and Kaback, H. R. (2001) Helix packing in the lactose permease of *Escherichia coli*: Distances between site-directed nitroxides and a lanthanide, *Biochemistry 40*, 3184−3188.
85. Voss, J., Hubbell, W. L., and Kaback, H. R. (1998) Helix packing in the lactose permease determined by metal-nitroxide interaction, *Biochemistry 37*, 211−216.

BI061195B